

This work was written as part of one of the author's official duties as an Employee of the United States Government and is therefore a work of the United States Government. In accordance with 17 U.S.C. 105, no copyright protection is available for such works under U.S. Law.

Public Domain Mark 1.0

<https://creativecommons.org/publicdomain/mark/1.0/>

Access to this work was provided by the University of Maryland, Baltimore County (UMBC) ScholarWorks@UMBC digital repository on the Maryland Shared Open Access (MD-SOAR) platform.

Please provide feedback

Please support the ScholarWorks@UMBC repository by emailing scholarworks-group@umbc.edu and telling us what having access to this work means to you and why it's important to you. Thank you.

Aerosol Layer Height With Enhanced Spectral Coverage Achieved by Synergy Between VIIRS and OMPS-NM Measurements

Jaehwa Lee^{ID}, N. Christina Hsu^{ID}, Andrew M. Sayer^{ID}, Colin J. Seftor^{ID}, and Woogyung V. Kim^{ID}

Abstract—This letter presents a near production-ready algorithm to retrieve the height of biomass burning smoke and mineral dust aerosols as part of National Aeronautics and Space Administration (NASA)’s Deep Blue aerosol data product suite. It utilizes the enhanced spectral coverage achieved by using colocated data from the Visible Infrared Imaging Radiometer Suite (VIIRS) and the Ozone Mapping and Profiler Suite Nadir Mapper (OMPS-NM), both aboard the Suomi National Polar-orbiting Partnership (S-NPP) satellite. In particular, the 412-nm top-of-atmosphere (TOA) reflectance from VIIRS and the ultraviolet aerosol index from OMPS-NM are used to determine the height and single-scattering albedo of the absorbing aerosols simultaneously. Constraints on aerosol optical depth at 550 nm and surface reflectance for the 412-nm band are provided by the operational VIIRS Deep Blue aerosol product. Wildfire smoke layer heights obtained from the algorithm over North America, where smoke plumes often stretched thousands of kilometers, are shown to agree with those from Cloud–Aerosol Lidar with Orthogonal Polarization (CALIOP) measurements, with an uncertainty generally within 1–1.5 km. This new height data set will be included in the upcoming Version 2 VIIRS Deep Blue aerosol product.

Index Terms—Aerosol, aerosol layer height (ALH), atmosphere, satellite.

I. INTRODUCTION

AEROSOLS play an important role in the earth system through interactions with solar and terrestrial radiation, clouds, and precipitation. These interactions have myriad implications for future climate [1], and since they take place in 3-D space, information on the vertical structure of aerosols,

in addition to their horizontal distribution, is essential for better quantification of these effects. Vertical structure near source regions is useful for the initialization/evaluation of aerosol injection height in aerosol transport models [2], and information downwind from source regions can be used for validation of transported aerosol height [3]. Surface particulate matter concentrations are strongly dependent on the vertical profile of aerosols [4], so knowledge of aerosol height is also important for air quality applications. Since all of these topics can benefit from the type of large scale, high spatiotemporal resolution data sets, which satellite-based sensors can provide, retrievals of such parameters from these sensors have been of great interest. This study focuses on retrieving aerosol layer height (ALH) using passive satellite sensors.

Satellite sensors have previously been used to provide ALH over large areas, in addition to aerosol optical depth (AOD) and (among other quantities) particle size in the total atmospheric column. Such techniques can be categorized into ones that employ active or passive instruments; the latter can further be divided into multispectral or stereo imaging. The Cloud–Aerosol Lidar with Orthogonal Polarization (CALIOP), arguably the most widely used data source to date for the vertical information, has provided detailed aerosol vertical profiles [5]. However, with a beam diameter of 70 m at the surface, it covers only limited part of the earth, directly along its orbit tracks, with a 16-day repeat cycle. Another widely used data set is produced from the Multi-angle Imaging SpectroRadiometer (MISR). MISR plume heights are determined using parallax applied to its multiangle imagery [6]. The stereoscopic (or multiangle) technique requires aerosol plumes to be visually discernable from the environment and so are more applicable (but not limited) to heterogeneous source plumes than more homogeneous downwind areas [7]. One of the advantages of this approach is that the retrieval accuracy is independent of uncertainties in optical properties of the plumes. However, with a swath width of only 360 km, MISR has nine-day global coverage at the equator. The dual-view Along-Track Scanning Radiometer (ATSR) instruments have also been used for stereo-based aerosol height retrieval [8], although ATSR’s swath width, around 550 km, was similar to MISR’s. Thus, these techniques all have a fairly limited sampling.

Recent efforts to retrieve ALH using single-view passive sensors, which in general have wider swath widths than the aforementioned instruments, opened the door to even broader spatial coverage. Examples include the O2 A/B-band [9], [10], O2–O2-band [11], thermal [12], and

Manuscript received February 21, 2020; revised April 8, 2020; accepted April 30, 2020. Date of publication May 14, 2020; date of current version May 21, 2021. This work was supported by the NASA Research Opportunities in Space and Earth Science (ROSES): The Science of Terra, Aqua, and Suomi NPP under Grant 17-TASNPP17-0015 and Solicitation NNH17ZDA001N-TASNPP. (Corresponding author: Jaehwa Lee.)

Jaehwa Lee and Woogyung V. Kim are with the Earth System Science Interdisciplinary Center (ESSIC), University of Maryland, College Park, MD 20740 USA, and also with the NASA Goddard Space Flight Center, Greenbelt, MD 20771 USA (e-mail: jaehwa.lee@nasa.gov; woogyung.v.kim@nasa.gov).

N. Christina Hsu is with the NASA Goddard Space Flight Center, Greenbelt, MD 20771 USA (e-mail: christina.hsu@nasa.gov).

Andrew M. Sayer is with the Universities Space Research Association, Columbia, MD 21046 USA, and also with the NASA Goddard Space Flight Center, Greenbelt, MD 20771 USA (e-mail: andrew.sayer@nasa.gov).

Colin J. Seftor is with Science Systems and Applications, Inc., Lanham, MD 20706 USA and also with the NASA Goddard Space Flight Center, Greenbelt, MD 20771 USA (e-mail: colin.seftor@ssaihq.com).

Color versions of one or more of the figures in this letter are available online at <https://ieeexplore.ieee.org>.

Digital Object Identifier 10.1109/LGRS.2020.2992099

1545-598X © 2020 IEEE. Personal use is permitted, but republication/redistribution requires IEEE permission.

See <https://www.ieee.org/publications/rights/index.html> for more information.

optical multispectral [13], [14] techniques. Each of these different approaches has their own strengths and limitations in terms of applicable aerosol types and optical depths, spatial resolution, and so on.

Here, we introduce the new, near production-ready Aerosol Single-scattering albedo and Height Estimation (ASHE) passive optical algorithm. As part of National Aeronautics and Space Administration (NASA)'s Deep Blue aerosol data product suite [15]–[17], ASHE will provide the height of biomass burning smoke and mineral dust aerosols; in this letter, an application to North American wildfire smoke aerosols is presented.

II. ASHE USING PASSIVE AND ACTIVE SENSORS TOGETHER

ASHE was originally designed to utilize data products from both passive and active sensors in its retrieval process, taking AOD and Ångström exponent (AE) from the Visible Infrared Imaging Radiometer Suite (VIIRS), ultraviolet aerosol index (UVAI) from the Ozone Mapping and Profiler Suite Nadir Mapper (OMPS-NM), and ALH from CALIOP [14], [18]. The algorithm was initially applied to the Moderate Resolution Imaging Spectroradiometer (MODIS) and the Ozone Monitoring Instrument (OMI) in place of VIIRS and OMPS-NM by Jeong and Hsu [13].

To retrieve ALH from ASHE, both the AOD and single-scattering albedo (SSA) need to be constrained since the UVAI is sensitive to both of them as well as ALH [19]. We utilize the 340–378-nm wavelength pair (at which ozone is nonabsorbing) for the UVAI

$$\text{UVAI}(\tau_a, \omega_0, z_a) = -100 \times \left\{ \log_{10} \left[\left(\frac{I_{340}}{I_{378}} \right)_{\text{meas}} \right] - \log_{10} \left[\left(\frac{I_{340}}{I_{378}} \right)_{\text{calc}} \right] \right\}$$

where τ_a , ω_0 , and z_a are AOD, SSA, and ALH, respectively, and I_{meas} and I_{calc} are the measured and calculated top-of-atmosphere (TOA) radiances. The Lambertian-equivalent reflectivity derived at the longer wavelength by matching the measured radiance is used for the calculated radiance at the shorter wavelength. Thus, the UVAI represents a deviation of measured radiance at 340 nm from its theoretical value calculated assuming wavelength-independent surface and aerosol contributions between the wavelength pair. For absorbing aerosols, UVAI increases with increasing AOD and ALH and with decreasing SSA.

In this earlier version of ASHE, the AOD was taken from the VIIRS Deep Blue aerosol product, and SSA was retrieved from UVAI using ALH along the CALIOP track as a constraint. Then, the algorithm assumed this SSA was spatially invariant across the entire (smoke or dust) aerosol layer. This enabled the expansion of ALH retrievals to the areas outside the CALIOP track by forward simulations of the UVAI with the given aerosol optical properties, finding the ALH providing a match to the observed UVAI. The retrieved ALH represents the radiatively effective height for the reflected sunlight, which is dependent on the extinction profile within the plume. Note

that appropriate aerosol optical models were incorporated to ensure spectral consistency of the AOD and SSA from the UV to the visible wavelength range. A detailed description of the original ASHE algorithm, including aerosol optical models used and the aerosol type detection method (among others), can be found in [14].

Through the above-described process, the retrieved SSA essentially served as a “scaling factor” for ALH retrievals. This means that the retrieval errors due to uncertainties in AOD and aerosol optical models were partially negated as the retrieved SSA along the CALIOP track exactly matches the observed ALH given AOD and UVAI. In other words, the accuracy of AOD and aerosol optical models had a limited impact on ALH retrievals, provided the errors are spatially consistent. Using UVAI as a measurement in the inversion meant that the application was limited to UV-absorbing aerosols with moderate to thick optical depths (>0.5 – 1.0 at 550 nm). In addition, the requirement for CALIOP further limited the application to those aerosol layers for which CALIOP-derived ALH is available.

III. ASHE USING PASSIVE SENSORS ONLY

Although the original ASHE delivered impressive spatial coverage, the ability to eliminate the need for CALIOP data would result in broader data coverage, as well as facilitate the implementation of ASHE in the operational Deep Blue aerosol algorithm suite [15]–[17]. Once ASHE and Deep Blue products are produced operationally together, they will both benefit from each other as, for example, Deep Blue surface reflectance can be used in ASHE and ASHE can provide ALH to Deep Blue. The increasing age of the CALIOP instrument was also a factor in developing an independent algorithm since VIIRS and OMPS-NM sensors will fly on the next four satellites in the Joint Polar Satellite System (JPSS) program and will provide data far beyond the lifetime of CALIOP. Note that the ALH product will be provided at the same spatial resolution as the VIIRS Deep Blue product (6×6 km at nadir), and the coarser-resolution UVAI from OMPS-NM ($50 \text{ km} \times 50 \text{ km}$ or $17 \text{ km} \times 17 \text{ km}$ at nadir depending on satellite) is linearly interpolated into the VIIRS pixels.

Given that CALIOP's role in the original ASHE was to provide a constraint on SSA, the main question that needs to be answered is whether ALH and SSA can simultaneously be retrieved only using spectral measurements from the passive sensors. To answer the question, we looked at the sensitivities of TOA reflectances at two VIIRS blue bands and the OMPS UVAI (340–378-nm pair) to ALH and 550-nm SSA (see Fig. 1). The simulation assumes a smoke optical model with an absorption AE (AAE) from the UV to the visible wavelength range of 2.0. Fig. 1(a) suggests that both 412-nm TOA reflectance and UVAI are strongly sensitive to ALH and SSA and are fairly orthogonal to each other, ensuring a large state vector domain over which an inversion can be made. Fig. 1(b) also shows results from the 490-nm band (not used in ASHE due to its usage for AOD retrievals in most cases), which reveal a smaller sensitivity to ALH due to weaker Rayleigh scattering. This stronger orthogonality between parameters implies that AOD derived from 490-nm reflectance

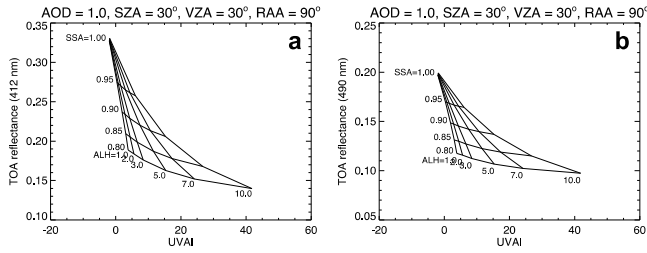


Fig. 1. Sensitivities of UVAI and TOA reflectances at (a) 412 and (b) 490 nm to ALH and SSA (550 nm) of smoke aerosols for a specific observation geometry and aerosol loading. A typical surface reflectance of 0.1 is assumed for both simulations. SZA, solar zenith angle; VZA, viewing zenith angle; RAA, relative azimuth angle.

(as in Deep Blue) has smaller uncertainties related to assumed height and, thus, smaller errors when propagated to retrieve ALH from the UVAI. In addition, Deep Blue dynamically assigns SSA as a function of geographic domain and AOD for optimal performance for smoke and dust, which can mitigate AOD errors due to SSA. It should be noted that 412-nm surface reflectance is available in the Deep Blue processing stream and will be used for ASHE retrievals.

Realistic aerosol optical models are another key requirement needed by the “passive-only” algorithm in order for it to perform well. The optical models assume a bimodal lognormal size distribution and are created as a function of fine-mode AOD fraction (FMF) and SSA both at 550 nm, and AAE (to determine spectral absorption; i.e., the imaginary part of the refractive index). The size distributions and real refractive indices used (see [14, Table 3]) are taken from Aerosol Robotic Network (AERONET) inversions [20], [21]. Nonspherical mineral dust particle shapes are accounted for by incorporating the same spheroid mixture as used in the AERONET inversion [22].

A significant effort is being made to systematically optimize the optical models used in each region for each aerosol type. The optimization is to better represent regional variations of aerosol properties, and at the same time, to substitute for the role that CALIOP data played in the original algorithm (i.e., providing a way for retrieval errors to be partially canceled). This is done by iteratively comparing the retrieved ALH to those from CALIOP and the original algorithm offline, and making necessary changes to the optical models until satisfactory similarity is found between the results. Through this process, optimal AAE and FMF are found within reasonable ranges for smoke and dust (AAE: 1.5 ± 0.5 for smoke or 2.5 ± 0.5 for dust, FMF: 0.9 ± 0.05 for smoke or 0.15 ± 0.05 for dust, cf. [23]). The values are then used to choose the appropriate lookup table in each region and aerosol type. These regional optimized values will be implemented before global data processing. AAE of 2.0 and FMF of 0.95 were found for North American wildfire smoke aerosols and are used in the analysis below.

IV. APPLICATION TO NORTH AMERICAN WILDFIRE SMOKE

This section demonstrates the initial performance of the passive algorithm for North American wildfire smoke aerosols.

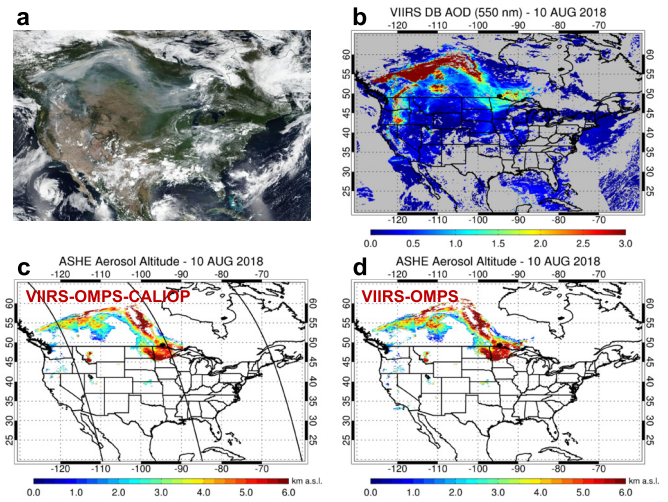


Fig. 2. Application of ASHE to a North American wildfire smoke event on 10 August 2018. (a) True color image from S-NPP VIIRS and (b) corresponding Deep Blue AOD at 550 nm are shown together with ALH from (c) original and (d) passive ASHE algorithms. Black lines passing from south to north in (c) are CALIOP tracks. ASHE is applied to smoke layers with AOD (550 nm) > 1.0.

Fig. 2 shows an application of both original and passive ASHE algorithms to the severe smoke event observed on 10 August 2018 using measurements from VIIRS and OMPS-NM, both onboard the Suomi National Polar-orbiting Partnership (S-NPP) satellite. The smoke layers across the continent mainly originated from multiple fire sources in the mountainous regions of British Columbia, Canada, and persisted for weeks [Fig. 2(a)]. Additional smaller fire sources were present over the western USA, including the states of Washington, Oregon, California, Idaho, Montana, and Utah. The 550-nm AOD of the smoke layers was comfortably higher than the application limit of ASHE (>1.0 in this case), even higher than 3.0 over vast areas [Fig. 2(b)]. ALH from ASHE suggests that significant portions of the smoke plumes were injected into the free troposphere (ALH > 3–6 km), enabling long-range transport stretching thousands of kilometers [Fig. 2(c) and (d)]. The close resemblance of ALH between the original and passive-only algorithms indicates the high caliber of the passive algorithm provided quality AOD and aerosol optical models are available. The passive algorithm also extends the spatial coverage to the latitudes greater than $\sim 60^\circ$, where the original algorithm failed to produce data due to CALIOP not overpassing the smoke plume in the specific granule. Note that ASHE, like Deep Blue, operates on a per-granule processing basis (every 6-min cut for VIIRS), not stitching consecutive granules together.

Fig. 3 shows the comparison of the ASHE-retrieved ALH for wildfire smoke layers over North America against results from CALIOP during Augusts from 2012 to 2018, a peak burning period. The CALIOP ALH is defined as the extinction-weighted mean height as an analog to what ASHE retrieves (radiatively effective height). Initial pixel-level collocations between the two data sets were made within 1 h in time and 6 km in space from each other. Only one ASHE retrieval for each across-track scan is chosen for each

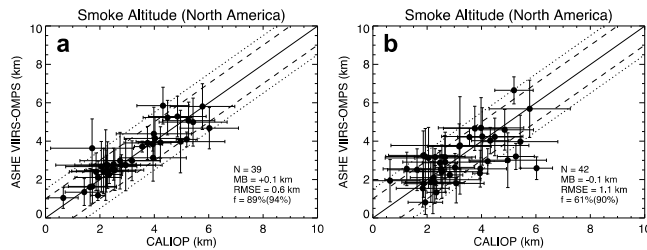


Fig. 3. Comparisons of ALH from (a) original and (b) passive ASHE algorithms against CALIOP for AOD (550 nm) > 1.0. Mean and standard deviation of colocated pixels for each transect across smoke layers are shown. Statistics shown are the number of data points (N), MB, RMSE, and fraction of data points (f) falling within 1 km (1.5 km).

CALIOP profile meeting the criteria. The comparisons were performed by averaging matched pixels for each transect across smoke layers, rather than for each pixel, since aerosols at high altitudes can move fast and the temporal differences (<1 h) can create significant artifacts. Shortening the temporal criterion severely decreases the number of samples compared because the two instruments are in different orbits, despite the close local solar equator crossing times [$\sim 13:30$ Coordinated Universal Time (UTC)].

We note that the passive algorithm only shows a slight decrease in performance compared to the original algorithm, with a mean bias (MB) of -0.1 versus 0.1 km (for the original algorithm) and root-mean-square error (RMSE) of 1.1 versus 0.6 km. The fraction of data falling within 1 km (1.5 km) of 61% (90%), together with the RMSE of 1.1 km, suggests that the one standard deviation error envelope is expected to be in a range $1\text{--}1.5$ km. The similar standard deviations between ASHE and CALIOP indicate consistent spatial variability between the two data sets. The larger number of data points obtained from the passive algorithm results from the algorithm making retrievals for some cases for which the original algorithm failed to do so. Much larger differences in data coverage are expected between the two algorithms in the real case (not restricted to the availability of CALIOP). Although not shown here, the comparison of a lower threshold AOD (550 nm) > 0.5 resulted in MB of -0.4 km, RMSE of 1.4 km, and fraction within 1 km (1.5 km) of 60% (84%), with a significantly increased number of data points ($N = 70$). The feasibility of extending the application limit to lower AOD will be addressed as part of the operational implementation effort, as better AOD retrievals will be available from the Version 2 Deep Blue algorithm.

The ALH retrieval errors are consistent with the theoretical values reported in our previous work [14] where we conducted error estimates due to various error sources, such as AOD, FMF, AAE, aerosol type, and so on. Uncertainties in SSA were found to be the largest source of error followed by aerosol type (smoke or dust) and AOD. Refer to [14] for a detailed description of the sources of errors and their magnitudes.

V. CONCLUSION

The ASHE, as part of NASA's Deep Blue aerosol algorithm suite, is poised to provide information on the height of biomass burning smoke and mineral dust aerosols over the globe.

By utilizing the enhanced spectral coverage achieved by the synergy between VIIRS and OMPS-NM as well as constraints by Deep Blue aerosol product, ASHE is now able to retrieve ALH without the need for CALIOP measurements. However, CALIOP still serves as an essential component of algorithm development by providing an invaluable validation target that can be used to optimize aerosol optical models for better performance. Initial assessment of ASHE for North American wildfire smoke events suggests a one standard deviation error envelope of $1\text{--}1.5$ km, which can be further improved in the future with the more accurate Version 2 Deep Blue AOD product (under development). The present algorithm is generic and can be applied to other sensors with similar capabilities, such as the Tropospheric Monitoring Instrument (TROPOMI) aboard the Copernicus Sentinel-5 Precursor and the Ocean Color Instrument (OCI) of the forthcoming Plankton, Aerosol, Cloud, ocean Ecosystem (PACE) mission. An application to geostationary satellite sensors is also possible, as next-generation imagers will be paired with UV-visible spectrometers (although a slight performance decrease is expected due to unavailability of the 412-nm band). The data set described in this work will be available as part of NASA's Version 2 VIIRS Deep Blue product, which is expected to be released in the near future.

ACKNOWLEDGMENT

The VIIRS, OMPS, and CALIOP science teams are acknowledged for their efforts to create and maintain the data records used in this investigation. This research was funded by NASA's radiation science program, managed by Hal Maring. More information about the Deep Blue aerosol project can be found at <https://deepblue.gsfc.nasa.gov/>.

REFERENCES

- [1] R. K. Pachauri and L. A. Meyer, *Climate Change 2014: Synthesis Report. Contribution of Working Groups I, II and III to the Fifth Assessment Report of the Intergovernmental Panel on Climate Change*. Geneva, Switzerland: IPCC, 2014, p. 151.
- [2] C. J. Vernon, R. Bolt, T. Canty, and R. A. Kahn, "The impact of MISR-derived injection height initialization on wildfire and volcanic plume dispersion in the HYSPLIT model," *Atmos. Meas. Techn.*, vol. 11, no. 11, pp. 6289–6307, Nov. 2018, doi: [10.5194/amt-11-6289-2018](https://doi.org/10.5194/amt-11-6289-2018).
- [3] E. P. Nowotnick, P. R. Colarco, E. J. Welton, and A. da Silva, "Use of the CALIOP vertical feature mask for evaluating global aerosol models," *Atmos. Meas. Techn.*, vol. 8, no. 9, pp. 3647–3669, Sep. 2015, doi: [10.5194/amt-8-3647-2015](https://doi.org/10.5194/amt-8-3647-2015).
- [4] A. van Donkelaar, R. V. Martin, and R. J. Park, "Estimating ground-level PM_{2.5} using aerosol optical depth determined from satellite remote sensing," *J. Geophys. Res.*, vol. 111, no. D21, 2006, Art. no. D21201, doi: [10.1029/2005JD006996](https://doi.org/10.1029/2005JD006996).
- [5] D. M. Winker *et al.*, "Overview of the CALIPSO mission and CALIOP data processing algorithms," *J. Atmos. Ocean. Technol.*, vol. 26, no. 11, pp. 2310–2323, Nov. 2009, doi: [10.1175/2009JTECHA1281.1](https://doi.org/10.1175/2009JTECHA1281.1).
- [6] D. Nelson, M. Garay, R. Kahn, and B. Dunst, "Stereoscopic height and wind retrievals for aerosol plumes with the MISR interactive explorer (MINX)," *Remote Sens.*, vol. 5, no. 9, pp. 4593–4628, Sep. 2013, doi: [10.3390/rs5094593](https://doi.org/10.3390/rs5094593).
- [7] R. A. Kahn *et al.*, "Wildfire smoke injection heights: Two perspectives from space," *Geophys. Res. Lett.*, vol. 35, no. 4, 2008, Art. no. L04809, doi: [10.1029/2007GL032165](https://doi.org/10.1029/2007GL032165).
- [8] D. Fisher, J.-P. Muller, and V. N. Yershov, "Automated stereo retrieval of smoke plume injection heights and retrieval of smoke plume masks from AATSR and their assessment with CALIPSO and MISR," *IEEE Trans. Geosci. Remote Sens.*, vol. 52, no. 2, pp. 1249–1258, Feb. 2014, doi: [10.1109/TGRS.2013.2249073](https://doi.org/10.1109/TGRS.2013.2249073).

- [9] S. Nanda *et al.*, "A weighted least squares approach to retrieve aerosol layer height over bright surfaces applied to GOME-2 measurements of the oxygen a band for forest fire cases over Europe," *Atmos. Meas. Techn.*, vol. 11, no. 6, pp. 3263–3280, Jun. 2018, doi: [10.5194/amt-11-3263-2018](https://doi.org/10.5194/amt-11-3263-2018).
- [10] X. Xu *et al.*, "Detecting layer height of smoke aerosols over vegetated land and water surfaces via oxygen absorption bands: Hourly results from EPIC/DSCOVR in deep space," *Atmos. Meas. Techn.*, vol. 12, no. 6, pp. 3269–3288, Jun. 2019, doi: [10.5194/amt-12-3269-2019](https://doi.org/10.5194/amt-12-3269-2019).
- [11] J. Chimot *et al.*, "An exploratory study on the aerosol height retrieval from OMI measurements of the 477 nm O₂-O₂ spectral band using a neural network approach," *Atmos. Meas. Techn.*, vol. 10, no. 3, pp. 783–809, Mar. 2017, doi: [10.5194/amt-10-783-2017](https://doi.org/10.5194/amt-10-783-2017).
- [12] A. Lyapustin, Y. Wang, S. Korkin, R. Kahn, and D. Winker, "MAIAC thermal technique for smoke injection height from MODIS," *IEEE Geosci. Remote Sens. Lett.*, vol. 17, no. 5, pp. 730–734, May 2020, doi: [10.1109/LGRS.2019.2936332](https://doi.org/10.1109/LGRS.2019.2936332).
- [13] M.-J. Jeong and N. C. Hsu, "Retrievals of aerosol single-scattering albedo and effective aerosol layer height for biomass-burning smoke: Synergy derived from 'A-Train' sensors," *Geophys. Res. Lett.*, vol. 35, no. 24, 2008, pp. L24801, doi: [10.1029/2008GL036279](https://doi.org/10.1029/2008GL036279).
- [14] J. Lee, N. C. Hsu, C. Bettenhausen, A. M. Sayer, C. J. Seftor, and M. Jeong, "Retrieving the height of smoke and dust aerosols by synergistic use of VIIRS, OMPS, and CALIOP observations," *J. Geophys. Res., Atmos.*, vol. 120, no. 16, pp. 8372–8388, Aug. 2015, doi: [10.1002/2015JD023567](https://doi.org/10.1002/2015JD023567).
- [15] N. C. Hsu, J. Lee, A. M. Sayer, W. Kim, C. Bettenhausen, and S. Tsay, "VIIRS Deep Blue aerosol products over land: Extending the EOS long-term aerosol data records," *J. Geophys. Res., Atmos.*, vol. 124, no. 7, pp. 4026–4053, Apr. 2019, doi: [10.1029/2018JD029688](https://doi.org/10.1029/2018JD029688).
- [16] A. M. Sayer, N. C. Hsu, J. Lee, C. Bettenhausen, W. V. Kim, and A. Smirnov, "Satellite ocean aerosol retrieval (SOAR) algorithm extension to S-NPP VIIRS as part of the 'Deep Blue' aerosol project," *J. Geophys. Res., Atmos.*, vol. 123, no. 1, pp. 380–400, Jan. 2018, doi: [10.1002/2017JD027412](https://doi.org/10.1002/2017JD027412).
- [17] A. M. Sayer, N. C. Hsu, J. Lee, W. V. Kim, and S. T. Dutcher, "Validation, stability, and consistency of MODIS collection 6.1 and VIIRS version 1 deep blue aerosol data over land," *J. Geophys. Res., Atmos.*, vol. 124, no. 8, pp. 4658–4688, Apr. 2019, doi: [10.1029/2018JD029598](https://doi.org/10.1029/2018JD029598).
- [18] J. Lee *et al.*, "Evaluating the height of biomass burning smoke aerosols retrieved from synergistic use of multiple satellite sensors over southeast Asia," *Aerosol Air Qual. Res.*, vol. 16, no. 11, pp. 2831–2842, 2016, doi: [10.4209/aaqr.2015.08.0506](https://doi.org/10.4209/aaqr.2015.08.0506).
- [19] N. C. Hsu *et al.*, "Comparisons of the TOMS aerosol index with sun-photometer aerosol optical thickness: Results and applications," *J. Geophys. Res., Atmos.*, vol. 104, no. D6, pp. 6269–6279, Mar. 1999, doi: [10.1029/1998JD200086](https://doi.org/10.1029/1998JD200086).
- [20] B. N. Holben *et al.*, "AERONET—A federated instrument network and data archive for aerosol characterization," *Remote Sens. Environ.*, vol. 66, no. 1, pp. 1–16, Oct. 1998, doi: [10.1016/S0034-4257\(98\)00031-5](https://doi.org/10.1016/S0034-4257(98)00031-5).
- [21] O. Dubovik *et al.*, "Application of spheroid models to account for aerosol particle nonsphericity in remote sensing of desert dust," *J. Geophys. Res.*, vol. 111, no. D11, 2006, Art. no. D11208, doi: [10.1029/2005JD006619](https://doi.org/10.1029/2005JD006619).
- [22] J. Lee, N. C. Hsu, A. M. Sayer, C. Bettenhausen, and P. Yang, "AERONET-based nonspherical dust optical models and effects on the VIIRS deep Blue/SOAR over water aerosol product," *J. Geophys. Res., Atmos.*, vol. 122, no. 19, pp. 10,384–10,401, Oct. 2017, doi: [10.1002/2017JD027258](https://doi.org/10.1002/2017JD027258).
- [23] P. B. Russell *et al.*, "Absorption angstrom exponent in AERONET and related data as an indicator of aerosol composition," *Atmos. Chem. Phys.*, vol. 10, no. 3, pp. 1155–1169, Feb. 2010, doi: [10.5194/acp-10-1155-2010](https://doi.org/10.5194/acp-10-1155-2010).